Assessment of radon fluxes at the Hyytiälä site from campaign and model data

Susana Barbosa[1], Ute Karstens[2], Xuemeng Chen[3], Claudia Grossi[4], Scott Chambers[5]

[1] INESC TEC, Portugal

[2] ICOS ERIC - Carbon Portal, Lund University

[3] University of Tartu

[4] Universitat Politècnica de Catalunya

[5] ANSTO, Australia

Abstract

Radon is an ideal passive atmospheric tracer. The use of radon as an atmospheric tracer requires knowledge on the radon flux from the earth's surface into the lower troposphere. Radon flux varies on multiple spatial and temporal scales, depending on both meteorological and surface conditions. The soil water content can be a critical factor for the estimation of radon fluxes from the surface, as it influences the transport of radon gas in the porous soil medium and its subsequent exhalation to the atmosphere. It is also a potential influence on gamma radiation dose rates, as the soil water content attenuates the propagation of gamma rays emitted by terrestrial radioisotopes in the subsurface layer. A campaign aiming to improve understanding on surface-atmosphere interactions influencing radon variability was performed at the SMEAR II station (Hyytiälä, Finland) in the framework of the transnational access project RELECT (Radioactivity and ELECTric field monitoring campaign at Hyytiälä). Detailed measurements of gamma radiation and soil radon concentration were performed from June to November 2017. These direct observations of ambient radioactivity are here analysed jointly with meteorological, surface, and flux data from the SMEAR II station, and with data from radon flux models.

1. Introduction

Radon (Rn-222) is a radioactive noble gas (half-life 3.8 days) generated mainly over land by radioactive decay of Radium (Ra-226) (Fig. 1). Unlike other radionuclides, which are bound to the soil or rock where they are formed, being a gas, radon is highly mobile and can be released into the atmosphere above. Emission of radon gas depends on local surface features, such as the radium content or the porosity and permeability of the radium-containing medium, which are stable for a given location. It is also very dependent on the multiple processes influencing the diffusive and advective movement of radon in the subsurface. Thus the emission of radon into the lower atmosphere is influenced by the meteorological conditions determining the medium's water content and the ability of radon to move within the subsurface and into the atmosphere above, which are highly variable in time. Gamma radiation is emitted from the earth's surface by radon's progeny as well as by terrestrial radionuclides (K, U, Th) in the sub-surface.

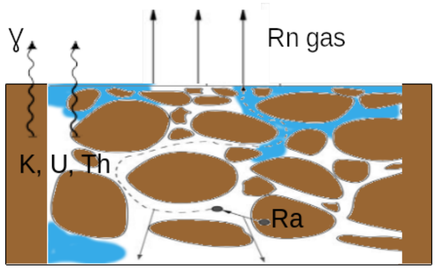

Fig. 1: Diagram illustrating the surface sources of radon and gamma radiation.

2. Campaign data

Radon gas concentration in the soil was measured at a depth of ~0.5m with a solid state silicon diode detector (Barasol BT45N, Algade Inc., France) detecting alpha particles between 1.5 MeV and 6 MeV (Barbosa, 2017a). The temporal variability of soil gas radon concentration is fairly stable up to early September displaying much larger oscillations in the autumn/winter (Fig. 2).

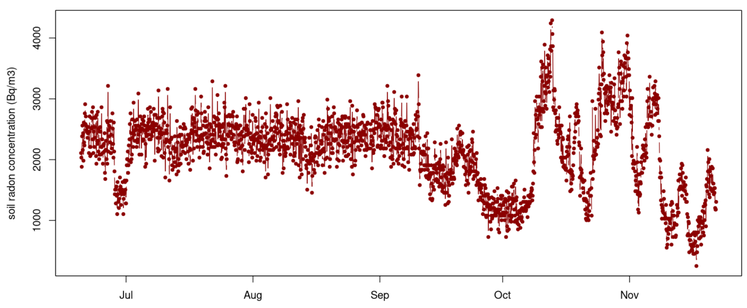

Fig. 2: Time series of radon gas concentration in the soil measured every 2 hours.

Gamma radiation was measured every 5 minutes with a 3"x 3" NaI(Tl) scintillator (Scionix, the Netherlands) detecting gamma radiation in the energy range from 475 keV to 3 MeV (Barbosa, 2017b). The time series of gamma radiation counts (Fig. 3) displays typical peaks due to precipitation scavenging. These peaks are removed using the 1-minute precipitation data available from the station. All values in the gamma radiation time series coincident with precipitation at the station are set to missing, as well as all the gamma radiation values in the following 3 hours after precipitation, in order to take into account radon's progeny decay time.

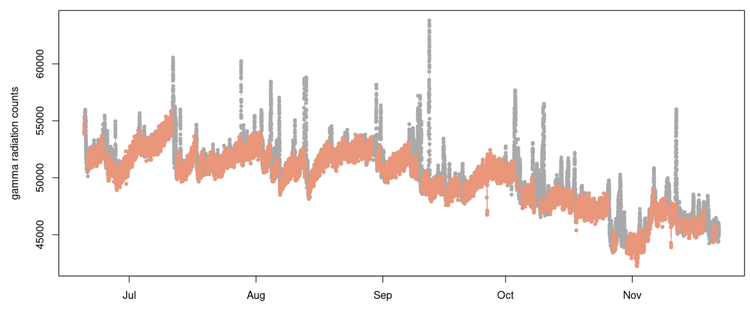

Fig. 3: Time series of gamma radiation counts (•) and after removal of the effect of precipitation (•).

3. Reanalysis and station data

3.1. Soil water content

The soil water content data include both station measurements and reanalysis data. Soil water content at 5 cm, 10 cm and 30 cm depths are obtained from the smartSMEAR database at the AVAA platform. Reanalysis data are obtained from reanalysis products ERA5-Land (Muñoz 2019) and GLDAS-Noah (Beaudoing & Rodell) at the gridpoint nearest to the Hyytiälä station. Comparison of station and reanalysis soil water content data shows substantial differences between station and reanalysis data, particularly for the Noah product (Fig. 4). Although ERA5 reanalysis is closer to the station data, the temporal variability of soil moisture at the site is not well represented by the reanalysis data (Fig. 5).

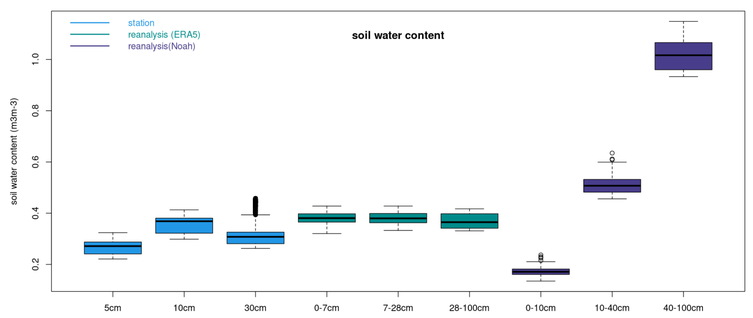

Fig. 4: Soil water content data distribution for station and reanalysis data.

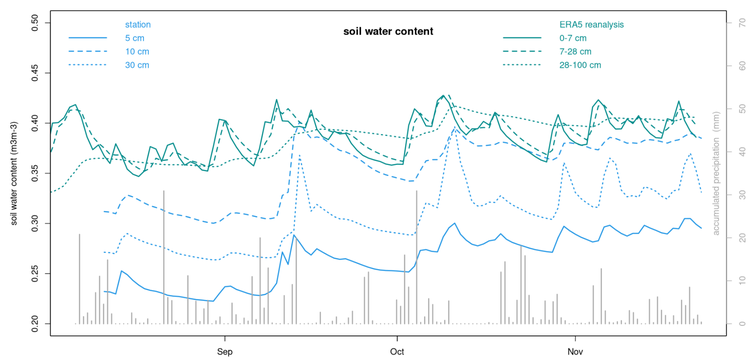

Fig. 5: Time series of station data and soil water content from ERA5 reanalysis.

Total gamma radiation counts are anti-correlated with soil water content (Fig 6), possibly due to the attenuation of gamma rays from terrestrial radionuclides on the ground and radon exhalation blockage in saturated soil. The residual gamma radiation time series is shown in Fig 7.

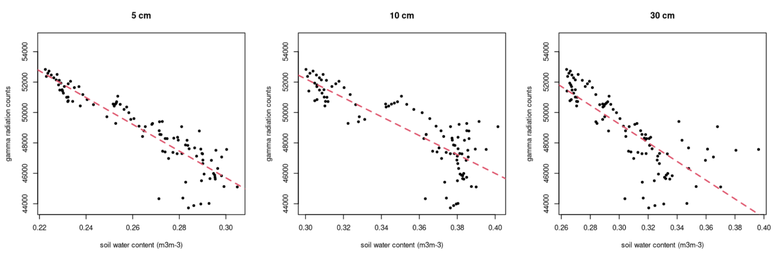

Fig. 6: Linear regression of daily-averaged gamma radiation counts and soil water content.

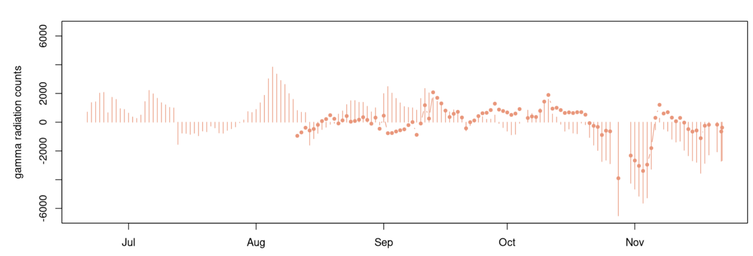

Fig. 7: Time series of gamma radiation counts residual's from linear regression on soil water content based on the available station data (•) and on ERA5 reanalysis data (|).

3.2. Snow

Snow fall data is obtained from the SMEAR II dataset and snow depth information (every 10 minutes) is obtained from FMI's station Juupajoki Hyytialä. Snow information from reanalysis products includes snow cover from the ERA5 product and snow depth from the Noah product. The data are displayed in Fig. 8 and show a good agreement between reanalysis and station data until early November, worsening afterwards. No direct correlation is found between soil gas radon concentration and the snow parameters for the period considered.

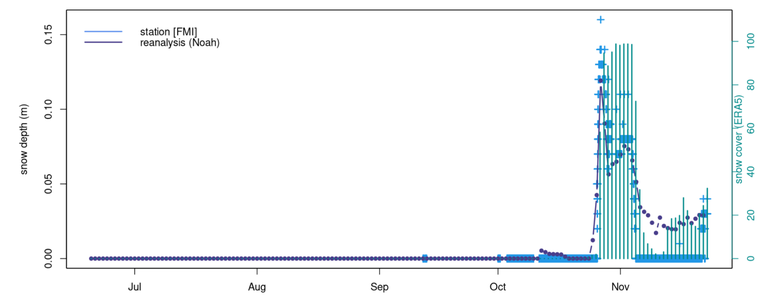

Fig. 8: Time series of snow depth and snow cover from station and reanalysis data.

3.3. Soil temperature

Soil temperature from reanalysis (Noah product) and from the SMEAR II dataset (Fig. 9) show a good agreement between station and reanalysis observations until mid-October, becoming increasingly distinct afterwards. The reanalysis soil temperatures exhibit larger variability than the station's soil temperatures. No direct correlation is found between soil gas radon concentration and soil temperature for the period considered.

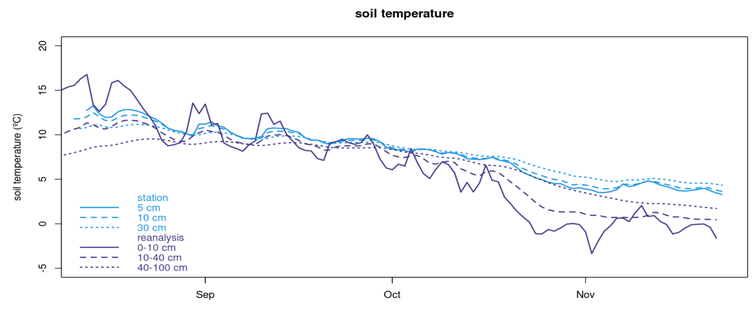

Fig. 9: Time series of soil temperature from station and reanalysis data.

4. Radon flux

Radon flux is computed based on the model of Karstens et al 2015, using as input soil parameters for the site and soil moisture from reanalysis data (Fig. 10). The resulting model-based time series of radon flux at the soil surface are displayed in (Fig. 11). Radon fluxes based on ERA5-Land and GLDAS-Noah soil moisture display a consistent temporal patterns both in terms of the overall trend and short-term variability. There is however a bias between the two radon fluxes, with the Rn flux computed from the GLDAS-Noah soil moisture being systematically higher than the Rn flux derived from ERA5-Land (Fig. 12).

- Diffusive transport of radon in the soil

$$D_e \frac{\partial^2 c(z)}{\partial z^2} - \lambda\, c(z) + Q(z) = 0$$

c ^{222}Rn activity concentration in soil air
λ radon decay rate
D_e effective diffusivity

- Production rate of radon in the soil

$$Q(z) = \lambda\ \rho_b\ c_{Ra}(z)\ \varepsilon(z)$$

c_{Ra} ^{226}Ra activity concentration in soil material assuming equilibrium between U and ^{226}Ra
ρ_b soil bulk density
ε emanation coefficient

- Effective diffusivity of radon in soil air

$$D_e = D_a \frac{(\theta_p - \theta_w)^2}{\theta_p^{2/3}}$$

D_a diffusion coefficient of radon in air
θ_p porosity
θ_w water filled pore space = soil moisture

Millington and Quirk (1960)

- Radon flux at the soil surface

$$j(z=0) = -Q\sqrt{D_e/\lambda}$$

Fig.10: Process-based radon flux model (Karstens et al, 2015).

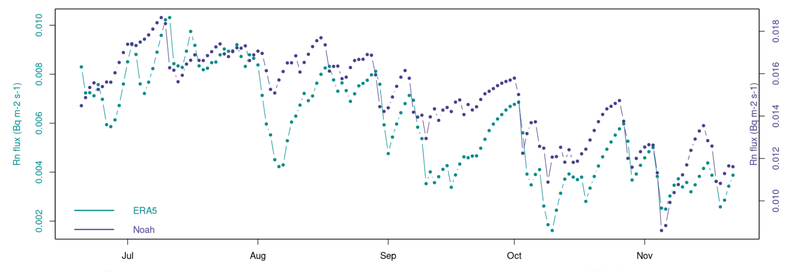

Fig.11: Time series of radon flux at the soil surface based on soil moisture from ERA5 and Noah products.

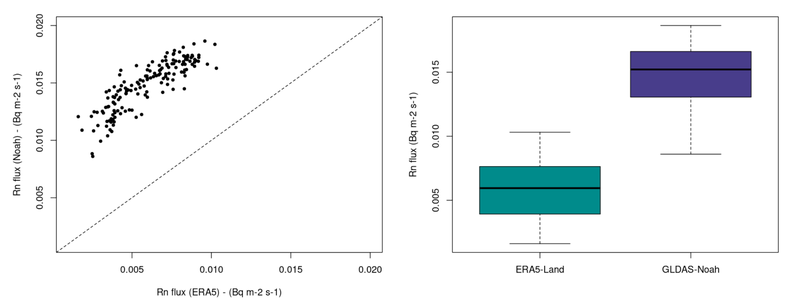

Fig.12: Radon flux from ERA5-Land versus radon flux from GLDAS-Noah products.

5. Conclusions

The temporal variability of gamma radiation is dominated by a downward trend associated with a corresponding increasing trend in soil moisture from summer to winter time.

After statistical modelling of the effect of soil water content, the main (negative) anomaly in gamma radiation coincides with the period of highest snow cover and snow depth, suggesting blocking of terrestrial gamma radiation from the ground.

Reanalysis data from ERA5 product is in better agreement with the station data than the Noah reanalysis product.

The agreement between reanalysis and station data is better in summer than winter.

The concentration of radon gas in the soil is stable during summer and exhibits large oscillations in the autumn/winter. It is not correlated with the modelled radon flux.

The variability of radon gas is influenced by the soil water content and snow cover, but the effect is difficult to observe directly from the data available no direct correlation is found between radon concentration in soil and the soil water content, temperature or snow.

Longer time series, covering at least several seasonal periods are needed to improve understanding of radon fluxes and improve parametrizations.

References

AVAA – Open Data Publishing Platform, https://www.fairdata.fi/en/avaa/, Accessed: [28 March 2018].

Barbosa, S, 2017a. Radon data from ENVRIplus TNA campaign RELECT at SMEAR II – HYYTIÄLÄ multi-disciplinary RI platform, https://doi.org/10.25747/JBVT-0940.

Barbosa, S, 2017b. Gamma radiation data from ENVRIplus TNA campaign RELECT at SMEAR II – HYYTIÄLÄ multi-disciplinary RI platform, https://doi.org/10.25747/JXKE-2J39.

Beaudoing, H. and M. Rodell, NASA/GSFC/HSL (2020), GLDAS Noah Land Surface Model L4 3 hourly 0.25 x 0.25 degree V2.1, Greenbelt, Maryland, USA, Goddard Earth Sciences Data and Information Services Center (GES DISC), Accessed: [12 October 2020], 10.5067/E7TYRXPJKWOQ.

Karstens, U., Schwingshackl, C., Schmithüsen, D., and Levin, I, 2015. A process-based 222radon flux map for Europe and its comparison to long-term observations, Atmos. Chem. Phys., 15, 12845–12865, https://doi.org/10.5194/acp-15-12845-2015.

Muñoz Sabater, J., (2019): ERA5-Land hourly data from 1981 to present. Copernicus Climate Change Service (C3S) Climate Data Store (CDS). (12 October 2020), 10.24381/cds.e2161bac.

Acknowledgements

Support provided by the SMEAR II station staff during the RELECT campaign is gratefully acknowledged.

This project 19ENV01 traceRadon has received funding from the EMPIR programme co-financed by the Participating States and from the European Union's Horizon 2020 research and innovation programme. 19ENV01 traceRadon denotes the EMPIR project reference.